LOW-FREQUENCY NOISE STUDY AND SURFACE WAVE ENHANCEMENT USING DATA FROM LARGE AND SMALL APERTURE ARRAYS

A.F.Kushnir, A.Dainty**, A.I.Gashin***, B.M.Shoubik**

** Moscow IRIS Data Analysis Center / SYNAPSE Science Center, Russia*
*** Air Force Phillips Laboratory, USA*
**** International Institute of Earthquake Prediction Theory, Russian Academy of Science*

Sponsored by AFOSR Special project SPC-94-4039

Abstract The detection and parameter estimation of surface waves originating from earthquakes and explosions are important procedures in nuclear test monitoring with seismic arrays, usually performed on a routine on-line basis. For small teleseismic and far regional events performing these procedures is often complicated because weak low-frequency surface waves from these events are as a rule registered against a background of temporally and spatially correlated seismic noise with a frequency spectrum overlapping that of the event surface waves. Low-frequency (LF) seismic noise has two explicit components: the first is transient and propagates as surface waves; the second has the features of a scattered field. The statistical properties of a LF noise field are affected by meteorological factors and vary in time.

In this work we investigated temporal and spatial features of the LF seismic noise below 0.5 Hz based on records of long period instruments of large and small aperture arrays: 6 z-componenl sensors of the NORSAR array, 11 similar sensors of the Grafenberg array, and 12 3-component very broad band sensors of the Geyokcha PASSCAL small aperture array. For assessment of noise field spatial correlation we evaluated noise coherence functions for array sensor pairs and implemented high resolution wide-band F-K analysis. The latter allows us to estimate azimuths and apparent velocities of the transient noise component of frequency (0.04-0.07) Hz which was observed at all the arrays and to confirm its origin as surface waves generated by sea shore surf. As an example, for the Geyokcha array the noise coherency for different sensors was to be greater than 0.8 in the frequency band (0.-1.) Hz. The transient LF noise component arrives at this array with apparent velocity about 4 km/sec and backazimuth pointing to the middle of the Caspian Sea. The LF noise component with a peak at frequencies about 0.2 Hz arrives at this array with very small incidence angles as scattered body waves.

The conventional beamforming method applied to LF array data for enhancement of weak teleseismic and far regional explosion surface waves sometimes failed to provide the expected increase in SNR. The reason is the noise coherence in the signal frequency band. This was the case for array data sets which we investigated. For example, for the Geyokcha array the beamforming did not give any noise suppression for frequencies below 0.8 Hz.

We have found that significant improvement in surface wave retrieval can be achieved by implementing adaptive group filtering (AGF) algorithms. We tested two versions of AGF: the optimal AGF (AOGF) which retains the signal waveform undistorted; and whitening AGF (AWGF) which distorts the signal but whitens residual noise and facilitates signal detection and onset time estimation. Both suppress the coherent noise component by taking into account the array noise matrix power spectral density (MPSD) estimated by multidimensional ARMA modeling.

Our experiments shows that AOGF and AWGF processing provides for l-componnent large aperture arrays significant improvements of explosion surface wave SNR in comparison with beamforming. The improvement is due to suppression of the transient LF noise component at frequencies (0.04-0.07) Hz and is especially large if the explosion and noise arrival azimuths are well separated. For the small aperture 3-component VBB array the AGF procedures allows retrieval of surface waves with SNR = 0.1 by suppressing not only the transient but also the scattered LF noise components in the frequency range (0.-1.) Hz. We have found that the generalization of the AGF method for 3-component array data processing gives new potential for retrieving signals from noise and estimating their parameters.

Keywords Adaptive statistical processing of array data; optimal group filtering; high resolution F-K analysis; suppression of coherent noise; retrieval of surface waves from noise

OBJECTIVE: Seismic monitoring with arrays under strong noise conditions: algorithms, techniques, system design and experimental data processing.

PRELIMINARY RESEARCH RESULTS: Algorithms and software have been developed for adaptive statistical array data processing. Current noise features are taking into account in this processing by periodic estimation of the array noise matrix spectral density. A special programming shell was designed for SUN workstations, providing a convenient tool for running multichannel processing programs in interactive and real time modes.

RECOMMENDATIONS AND FUTURE PLANS: We recommend the wide use of VBB 3-component small aperture arrays, which are the most effective instruments for seismic monitoring. Our plan is to develop a modern adaptive statistical software for these array data processing.

Properties of low frequency noise fields. Detection and parameter estimation of surface waves originating from earthquakes and explosions are important procedures in nuclear test monitoring with seismic arrays, usually performed on a routine on-line basis. The effectiveness of these procedures impacts on the accuracy of small-events source location and on identification based on single array data[1]. Measurement of surface wave magnitudes is an effective means for the explosion yield evaluation [2].

For small teleseismic and far regional events, performing these procedures is often complicated, because weak low frequency surface waves from these events are, as a rule, being registered against a background of a temporally and spatially correlated seismic noise with a frequency spectrum overlapping that of the event surface waves. Low-frequency (LF) seismic noise has two explicit components with peaks at frequencies (0.04-0.07) and 0.2 Hz. The first is a transient propagating as a surface wave, the second is due to scattered noise field features. Both are assumed to originate from ocean storm activity but possess different mechanisms of transition to seismic energy. The serious nuisance for signal processing is that statistical properties of the LF noise field, namely temporal and spatial correlation features, are affected by meteorological factors and vary in time.

Optimal group filtering. The main procedures of conventional array data processing are beamforming and broad-band F-K analysis [3]. The first is implemented for refining from noise seismic phase waveforms that facilitate the subsequent phase parameter measurment, the second for estimating slowness vectors of signal waves. In practice these procedures do not provide the expected efficiency: for large aperture arrays, mainly due to the signal incoherence caused by medium inhomogenities; for small aperture arrays due to noise coherence (noise spatial correlation).

The generalized beamforming method [4] allows us to improve the signal waveform refinement in the case of coherent noise [5,6]. This method can be described as a group filtering of array data using the filter with the vector frequency response (VFR)

$$g^*(f,p) = h^*(f,p)\, F^{-1}(f) / [h^*(f,p)\, F^{-1}(f)\, h(f,p)],$$

where $h(f,p)$ is the vector of phase shift factors $h_j(f,p)=\exp\{-i2\pi f p^* r_j\}$, $j=1,...,m$, which are determined by the array sensor coordinate vectors r_j and a signal wave slowness vector $p=(p_x,p_y)$;

* denotes the Hermitian conjugation. A group filter (GF) transforms a vector spectrum $x(f)$ of m-channel array time series into a spectrum $y(f)$ of output scalar time series by the equation $y(f) = g^*(f,p)\, x(f)$. The GF with the VFR $g(f,p)$ is the statistically optimal one (OGF) because it takes into account the array noise matrix power spectral density (MPSD) $F(f)$. Conventional beamforming can be treated as a group filtering with VFR $g(f,p)$, where $F(f) = I$, I is the identity matrix.

The optimal group filtering method can be extended for 3-component (3C) array data processing [7]. In this case $x(f)$ is a $3m$-dimensional vector spectrum of m 3C array traces, $F(f)$ is a MPSD of a 3C array noise, the vector $h(f,p)$ is composed of m 3C vectors $h^\circ_j(f,p) = h_j(f,p)b(p)$, where $b(p)$ depends on the type of a treated wave phase. In particular, for Raleigh surface waves, $b(p) = i \sin\psi\, (p_x, p_y, -i|p|ctg\psi)^*/|p|$, where ψ depends on the ellipticity of the Raleigh wave [8].

The efficiency of a practical application of the OGF is influenced by the method used for the estimation of the noise MPSD $F(f)$. For this purpose, we propose multidimensional ARMA modeling of array noise records preceding the event. The OGF with the VFR $g(f,p)$, containing such an estimated noise MPSD we call adaptive OGF (AOGF). Beamforming and AOGF are procedures that do not distort a signal waveform.

A useful modification of the AOGF is an adaptive noise whitening group filter (AWGF), which produces a white residual noise output and in many cases provides the highest output SNR, but distorts the signal [6]. The AWGF has the frequency response $w^*(f,p) = h^*(f,p)\, F^{-1}(f) / [h^*(f,p)\, F^{-1}(f)\, h(f,p)]^{1/2}$.

Estimation of wave apparent slowness. Coherent LF noise can sometimes be a significant hinderance for estimating slowness of weak surface waves by the conventional broad band F-K analysis. It is especially so if the number of sensors and/or the array aperture are small. We found that in this case, some improvement can be achieved if we use high resolution (HR) F-K analysis, which consists of mapping over slownesses $(p_x p_y)$ the function

$$P(p) = [\, h^*(f_0,p)\, F^{-1}(f_0)\, h(f_0,p)]^{-1},$$

where $F(f)$ is the ARMA estimate of a MPSD of array records. The vector $\mathbf{p}^\blacklozenge$ corresponding to a maximum of the map $P(p)$ represents the wave slowness estimate. The smoothness over frequency of an ARMA model (which in practice is calculated using low orders) implies that $\mathbf{p}^\blacklozenge$ is really a wide band estimate averaged over some frequency band around f_0.

There exist maximum likelihood (ML) algorithms for the slowness estimation of signal waves obscured by a spatially correlated noise. A ML algorithm derived under the assumption that nothing is known about a signal waveform consists of the evaluation of a vector $\mathbf{p}^\blacklozenge$ which maximizes the function

$$Q(p) = \Sigma\, |\, h^*(f,p)\, F^{-1}(f)\, x(f)|^2 / [h^*(f,p)\, F^{-1}(f)\, h(f,p)],$$

where summation is made in f over an assigned frequency band around f_0 [7]. This theoretical formulation allows us to suggest an adaptive algorithm for wave slowness estimation under conditions of strong coherent noise. It consists of the mapping over slownesses $(p_x p_y)$ the

function $Q(p)$ where $x(f)$ are spectra of signal wave array records, $F(f)$ is the ARMA estimate of the noise MPSD calculated using preceding array noise observations.

Study of LP large aperture array records. We investigated characteristics of LF noise and efficiency of slowness estimation and SNR enhancement of surface waves using records of long period (LP) instruments of the large aperture NORSAR and Grafenberg arrays. Table 1 shows the characteristics of the analyzed data sets containing explosion surface wave seismograms and noise records at preceding and subsequent time intervals.

Table 1. Characteristics of LP array data sets

Data set	1	2	3	4
Array	NORSAR	NORSAR	NORSAR	GRAFENBERG
LP sensors	6 z-comp	6 z-comp	5 z-comp	11 z-comp
Day of observation	30.05.83	27.10.84	27.12.81	26.10.83
Wave azimuth (degrees)	78°	105°	75°	61°
Wave velocity (km/s)	3.5	3.6	3.6	3.7
Data interval (sec)	7200	5400	6000	2700
Signal onset time (sec)	4500	2700	3700	1300
Sampling rate (Hz)	1	1	1	1

Figs 1- 4 illustrate the processing results for these data sets. Fig. 1 shows the power spectral density (PSD) and coherence function of signals and noise registered at NORSAR. We see that, for all three records, taken in different seasons of the year, the noise PSD exhibits a strong peak at frequencies (0.04-0.06) Hz (Fig. 1,c), which overlaps with dominant frequencies of the surface wave signal (Fig. 1,d). This NORSAR noise component preserves rather strong coherence over the total array aperture (Fig. 1,e): for the sensors NA1 and NC4 having separation 47 km (Fig. 1,a), the coherence is above 0.6. The HR F-K analysis (Fig. 2,c and Fig. 3,d) shows that the NORSAR noise component in the frequency band around 0.05 can be treated as a transient propagating with apparent velocity about 3.5-4.0 km/sec, typical for surface waves. Note that the estimated propagation azimuths of these noise waves support the supposition that the waves are generated by surf at sea shores: at the Baltic Sea for data sets 1, 2 (Fig. 2,c) and at the North Sea for data set 3 (Fig. 3,d).

The noise component with peak frequency 0.2 Hz does not exhibit coherency (Fig. 1,e); this corresponds with its conventional representation as a scattered noise field. The explosion surface waves registered by NORSAR demonstrate rather good coherence: more than 0.8 over the total array aperture (Fig. 1,f).

Explosion surface waves in the data sets 1 and 2 have small SNR. For this reason, the signal processing was performed here after filtering the data in the frequency band (0.-0.1) Hz with the help of a high quality Chebyshev filter (Fig. 1,b). This increases SNR by suppressing the 0.2 Hz noise component. Note that signal processing of these data sets is also impeded by the small difference between the noise and signal wave arrival directions: noise azimuths in both cases are about 40-50° (Fig. 2,c), signal azimuths are 78° for event 1 and 105° for event 2.

Apparently for the above reasons, the F-K analysis of the signals does not provide a reliable estimation of the signal azimuths and apparent slownesses: the estimated values vary rather strongly with changes in the parameters of the HR F-K algorithm.

Figs 2,a and 2,b show the results of processing the data sets 1 and 2 with the help of beamforming (trace 1), AOGF (trace 2), and AWGF (trace 3) procedures. Trace 4 in each figure is a record of the first array sensor. Figs 2,d and 2,e show the PSDs of the traces mentioned. We see that, by taking into account the noise coherence, the AOGF provides in these examples a rather significant addition to the beamforming suppression of the transient noise in the frequency band (0.05-0.08) Hz. The AWGF traces demonstrate the potential of this method for enhancement of the accuracy of surface wave onset time estimation.

The data set 3 was processed in both initial (0.-0.5) Hz (Fig. 3,a) and LP-filtered (0-0.1) Hz (Fig. 3,b) frequency bands. For this data, signal and noise arrival directions are quite different (76° and 315°,) and the HR F-K analysis provides satisfactory accuracy and stability (Figs 3,c and 3,d). The adaptive group filtering performance (Figs 3,a; 3,b and 3,e) is also better than in the previous cases. It is seen from Fig. 3,e that the AOGF provides significant suppression of noise components in comparison with beamforming up to 0.2 Hz. After processing in the frequency band (0.-0.1) Hz, the Rayleigh phase waveform emerges explicitly in the AOGF trace and the low frequency start of the signal is emphasized in the AWGF trace, allowing exact estimation of the signal onset time.

Data set 4 contains records made at 11 long period sensors of the large aperture Grafenberg array. The array is located away from a sea shore, but the features of low frequency noise here are remarkably similar to those for NORSAR. One can clearly see this, if one compares the noise PSD in Fig. 4,e ('GR1' curve) with that in Fig. 1,e ('NA1-ev.3' curve) and the noise HR F-K diagram in Fig. 4,d with that in Fig. 3,d. From the signal and noise HR F-K maps (Figs 4,a and Fig. 4,B), arrival azimuths of the signal and transient noise are quite different for this data set (60° and 314 °). For this reason, the AOGF provides a significant addition to the beamforming enhancement of SNR in a wide frequency band (0.-0.5) Hz (Fig. 4,e). The greatest noise suppression is achieved for (0.05-0.08) Hz transient noise components, but some suppression is visible for scattered components around 0.2 Hz. In Figs 4,a and 4.b results of the AOGF and AWGF performance in the frequency bands (0.-0.5) Hz and (0.-0.1) Hz demonstrate that the method can be really useful for processing LF surface waves registered by large aperture arrays.

Study of VBB small aperture array records. The well-tested NORESS-type small aperture arrays are essentially oriented to regional seismic monitoring and are equipped with short period instruments recording seismic energy above 0.5 Hz. They contain only one central long period sensor. For this reason, there are not many studies of low-frequency noise field coherency in the limits of these array aperture. The α-stations of the International Monitoring Network currently being deployed could be designed as 3-component wide band small aperture arrays containing about ten very broad band (VBB) 3C sensors within an aperture about 1.5 - 3 km [9]. Prototypes of such stations have been tested in the framework of the PASSCAL program; for example, the VBB subarrays of the Pinyon Flat (USA) and Geyokcha (Turkmenia) experimental arrays can be treated as such prototypes. Fig. 5,d shows the configuration of the

VBB subarray of the Geyokcha array deployed not far from Turkmenia capital Ashgabad (latitude 37.93°, longitude 58.11°). It has been recording during 93 and 94. The array was situated on thick sedimentary rocks and hence was affected by intense seismic noise.

The typical PSD of the Geyokcha noise is shown in Fig. 5,e for the frequency range (0.-10.) Hz and in more detail in Fig. 5,f for the frequency range (0.-1.) Hz. We see that the PSD has four peaks at frequencies 0.07, 0.2, 1.5 and 4.5 Hz. In Fig. 5,e, the noise PSD for the central sensor Z-instrument is compared with the PSD of a beam composed from noise records of all 12 VBB Z-instruments. The beam is steered to surface waves originating from the Chinese Lop Nor Test Site (azimuth 71.7°, app. velocity 3.55 km/sec). We see that the noise below 1. Hz is not suppressed by the beamforming procedure. This indicates that the noise field is highly spatially correlated for these frequencies. Fig. 6,d shows noise coherence functions for two closely located (B32, C22) and two more widely spaced separated (NHB, SEH) Z-sensors of the array. We see that for the first case coherencies are very close to 1 over all the frequency band (0.-1.) Hz, and for the second case have values larger then 0.8 up to 0.3 Hz. The HR F-K analysis for the strongest spectral peak at 0.2 Hz (Fig. 5,a) revealed that this noise component can be regarded as composed of body waves arriving with very low incidence angles. In the light of the thick sedimentary layer beneath the array this does not contradict the description of this component as a scattered field. The HR F-K map for the other LF noise peak at (0.05-0.07) Hz (Fig. 5,b) shows that this noise component is composed of surface waves arriving from the Caspian Sea.

Due to the small aperture and the high correlation of noise for different sensors, one may erroneously conclude that the Geyokcha type VBB array is a bad instrument for analyzing teleseismic and far regional surface waves. Really, the beamforming method does not provide any improvement in SNR for these waves and their F-K analysis is hampered by the coherent LF noise. To demonstrate the applicability of the AOGF method for this case, we simulated explosion surface wave seismograms (in the form of Berlage pulses with mean frequency 0.06 Hz and duration of 150 sec shifted in time as if originating from the Lop Nor Test Site) and mixed them with real Z-component records of Geyokcha VBB array noise. This model mixture (with the power SNR=0.1) was processed by the AOGF in the frequency band (0.-1.) Hz. The results shown in Figs 5,c and 5,f allow us to assert that the AOGF has in this case great potential: the signal SNR was improved 40 times due to effective suppression of not only transient (0.06 Hz) but also scattered (0.2 Hz) noise components (Fig. 5,f).

Fig. 6 illustrates results of an implementation of the **3-component** version of the AOGF procedure for enhancing surface waves in seismograms of the Chinese nuclear test of 10.06.94. We had for experimental processing records of only six 3C STS-2 seismometers (marked in Fig. 5,c by crosses).

Fig. 6,c shows the noise PSDs for N, E, and Z components of the central VBB sensor. Interesting here is the similarity of all spectra for frequencies above 0.05 Hz and great differences between the spectra of the vertical and horizontal components below 0.05 Hz. The latter can be explained by the likely origination of this noise fraction from wind impact on the Earth's surface unevenness.

The 3C seismogram of the Lop Nor nuclear test is shown in Fig. 6,a. Figs 6,b, and 6,e exhibit the results of processing the six 3C explosion seismograms (18 channels) by the 3C

versions of the beamforming and AOGF procedures (for the band [0.-1.] Hz). We see that the beam steered to the azimuth and velocity of Lop Nor explosion surface waves does not enhance these waves and passes through the bulk of the P-wave energy. In contrast, the similarly steered AOGF remarkably extracts explosion surface waves and suppresses the P-wave and its coda. Note that the noise suppression is strongest for the (0.01-0.03) and (0.1-0.5) Hz bands.

The experiments made with the Geyokcha array LF signal and noise records allow us to assert that VBB small aperture arrays can serve not only as the best instruments for regional seismic monitoring but also as a good tool for measurements of surface wave parameters for teleseismic and far regional events.

Acknowledgments

We thank Dr. D. Harvey (JSPC, Boulder, Colorado, USA) who delivered the Geyokcha array data set with seismograms of the China nuclear test of 10.06.94 to the Moscow IRIS Data Analysis Center.

References

1. S. Mykkeltveit, F. Ringdal, T. Kvarna and R. Alewine, 1990. Application of regional arrays in seismic verification. *Bull. Seism. Soc. Am., vol. 80, p.1777-1800.*

2. R.A. Hansen, F. Ringdal, P.G. Richards, 1990. The stability of RMS L-measurements and their potential for accurate estimation of the yields of Soviet underground nuclear explosions. *Seism. Soc. Am., vol. 80, p. 2106-2126*

3. S.Mykkeltveit and H. Bungam, 1984. Processing of regional events using data from small-aperture arrays. *Bull. Seism. Soc. Am., vol. 74. p. 2313- 2333.*

4. J. Capon, 1970. Application of space-time domain decision and estimation theory to antenna processing system design. *Proc. IEEE, vol. 58, p. 1170-1181.*

5. J.P. Claassen, 1992. The application of multiply constrained minimum variance adaptive beamforming to regional monitoring. *Bull. Seism. Soc. Am., vol. 82, p. 2191-2212.*

6. A.F. Kushnir, 1995. Algorithms for adaptive statistical processing of seismic array data. *Proceedings of NATO Advanced Study Institute on Monitoring of a Comprehensive Test Ban Treaty, Portugal 1995. Kluwer Pub. Comp., Amsterdam.*

7. A.F. Kushnir (ed.), 1995. Seismic monitoring with small aperture arrays under strong noise conditions: algorithms, technique, system design and experimental data processing. *Technical report on EOARD special project SPC-94-4039.*

8. K. Aki, P. Richards, 1980. Quantitative seismology. Theory and Methods, *Freeman and Co., San Francisco.*

9. Prototype Arrays Incorporate New Technologies and Reduce Costs, *The Monitor, Newsletter of the Nuclear Monitoring Research Office, ARPA, Vol. 4/No 2, 1994*

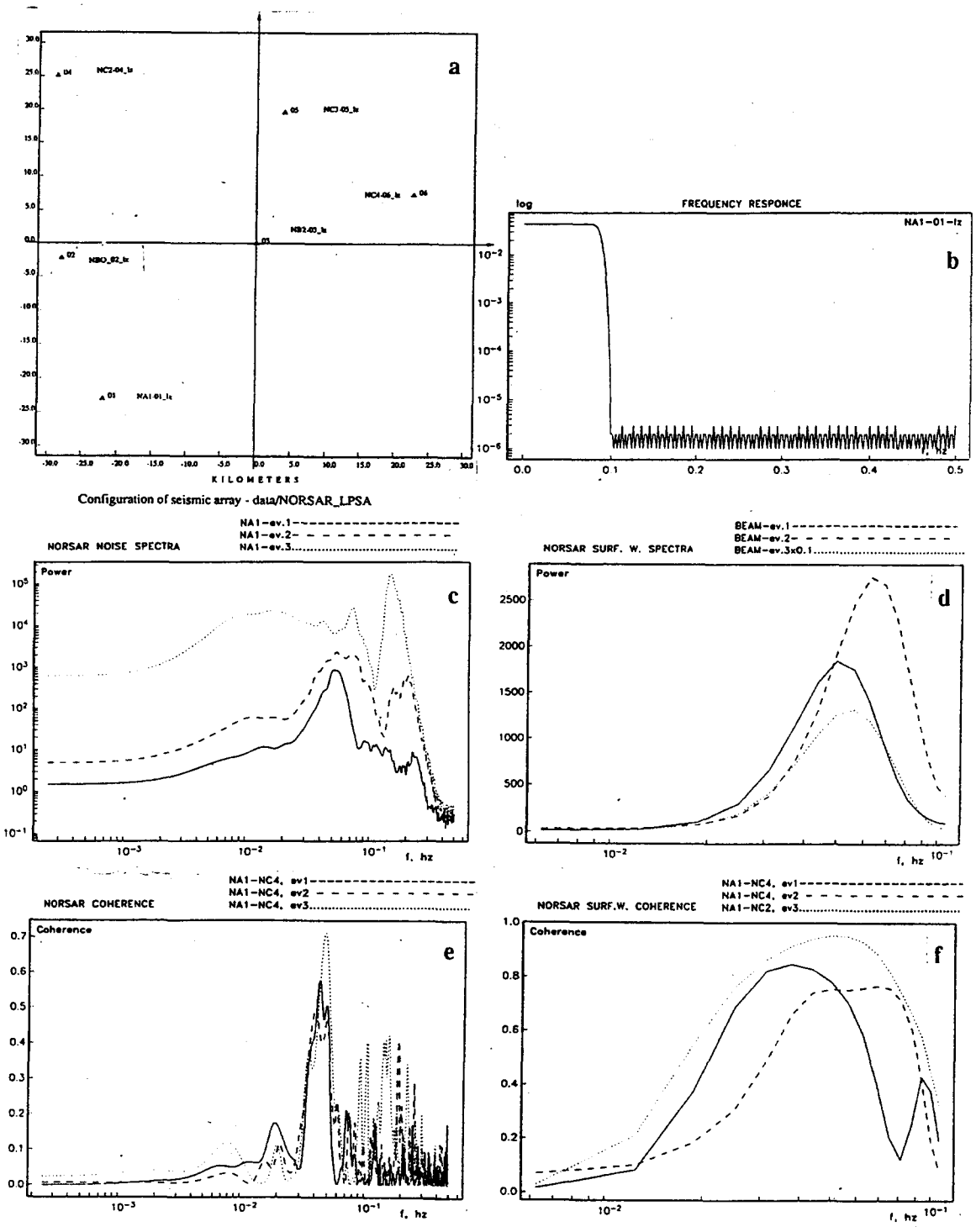

Fig. 1. NORSAR LP noise and signal characteristics: a) the location of NORSAR LP sensors; b) the Chebyshev filter response; c) the PSD of NORSAR LP noise; d) the PSD of explosion surface waves; e) the noise coherence functions; e) the coherence functions of explosion surface waves.

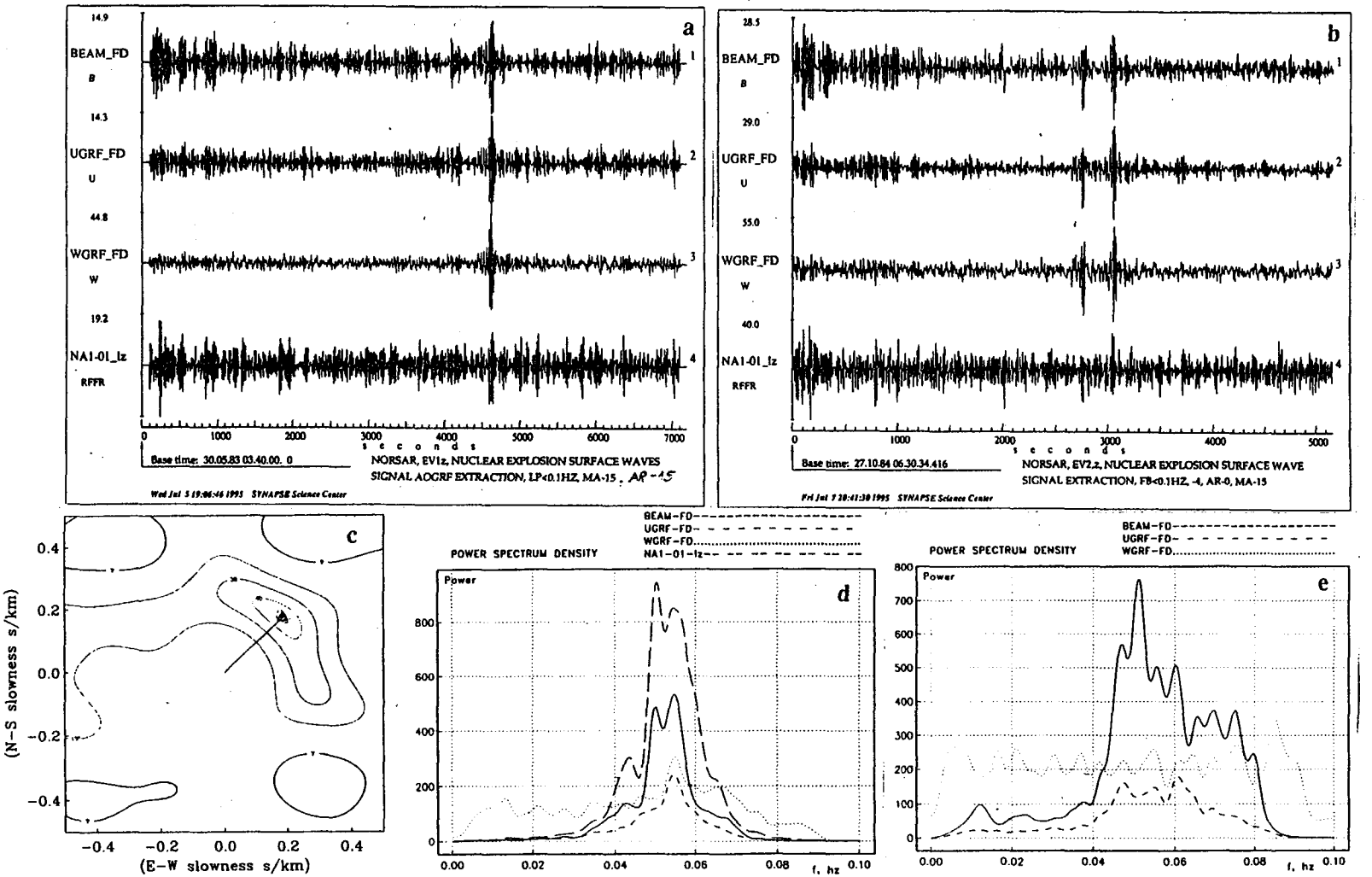

Fig. 2. Adaptive processing of NORSR data sets 1 and 2:
a), b) the extraction of surface wave by the adaptive group filtering (AGF);
c) the noise F-K map; d), e) the noise suppression by the AGF.

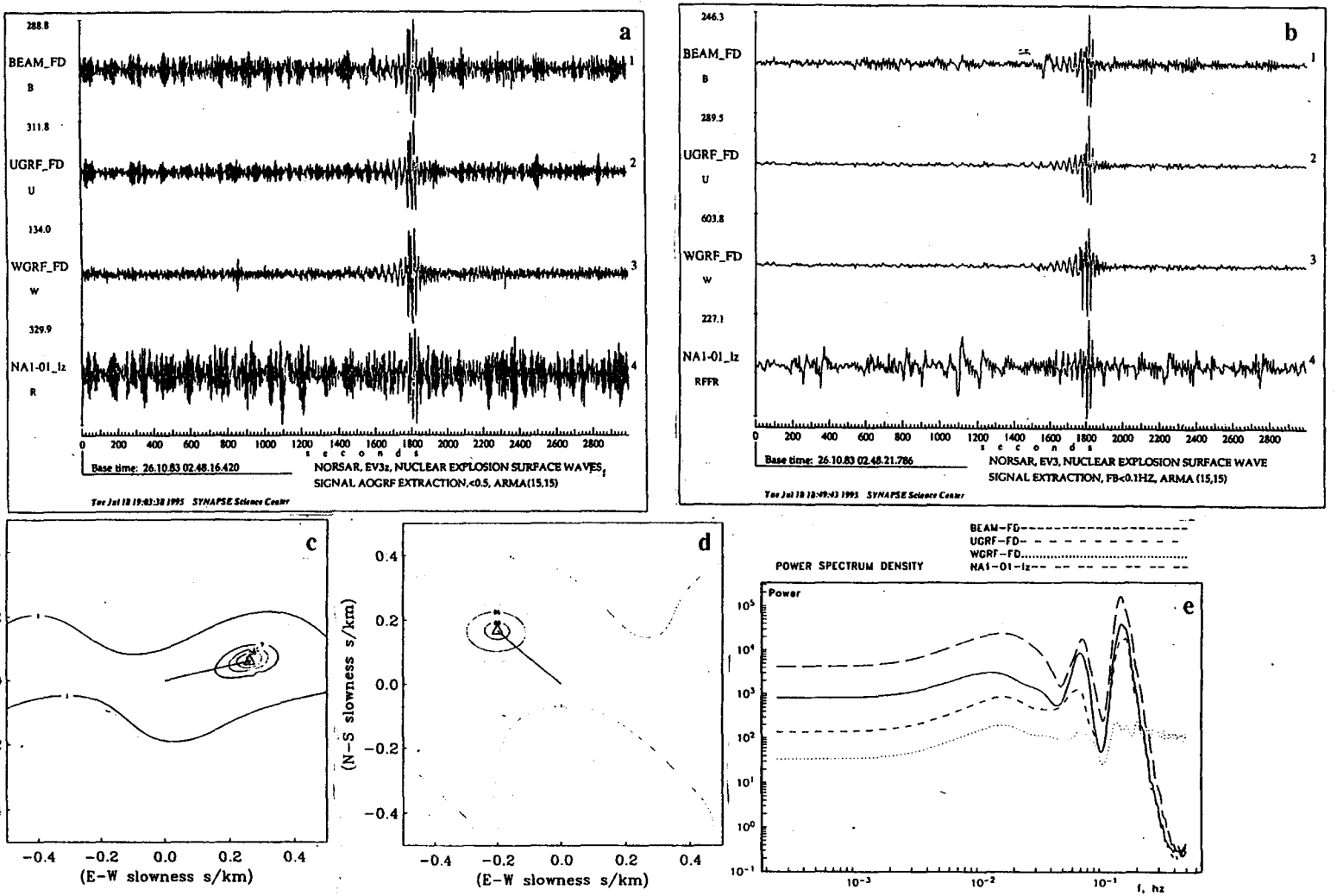

Fig. 3. Adaptive processing of NORSAR data set 3:
a), b) the extraction of surface waves by the adaptive group filtering (AGF) in the frequency ranges (0.-0.5) Hz and (0.-0.1) Hz;
c),d) the signal and noise F-K maps; e) the noise suppression by the AGF.

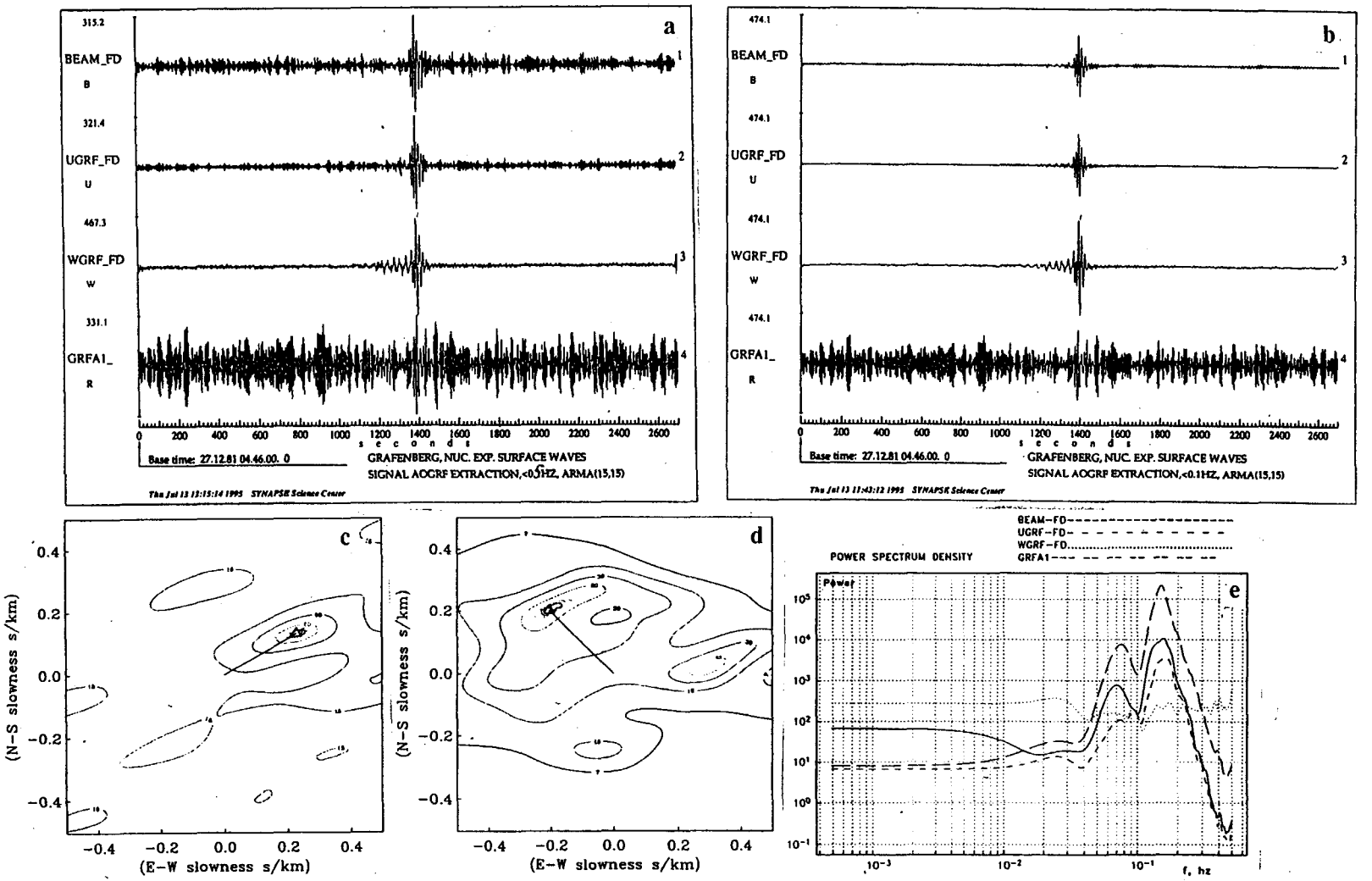

Frequency = 0.060 Hz, HIGH RESILUTION Azim. of max= 60.15 Ap. vel. of max= 3.78 Adapt. AR order IP=15 Adapt. MA order IQ= 0 Regulariz.=.0100000 Adapt. mode =-2

Frequency = 0.060 Hz, HIGH RESILUTION Azim. of max= 314.64 Ap. vel. of max= 3.49 Adapt. AR order IP=15 Adapt. MA order IQ= 0 Regulariz.=.0100000 Adapt. mode =-2

Fig. 4. Adaptive processing of the GRAFENBERG data set:
a), b) the extraction of surface waves by the adaptive group filtering (AGF) in the frequency ranges (0.-0.5) Hz and (0.-0.1) Hz;
c),d) the signal and noise F-K maps; e) the noise suppression by the AGF.

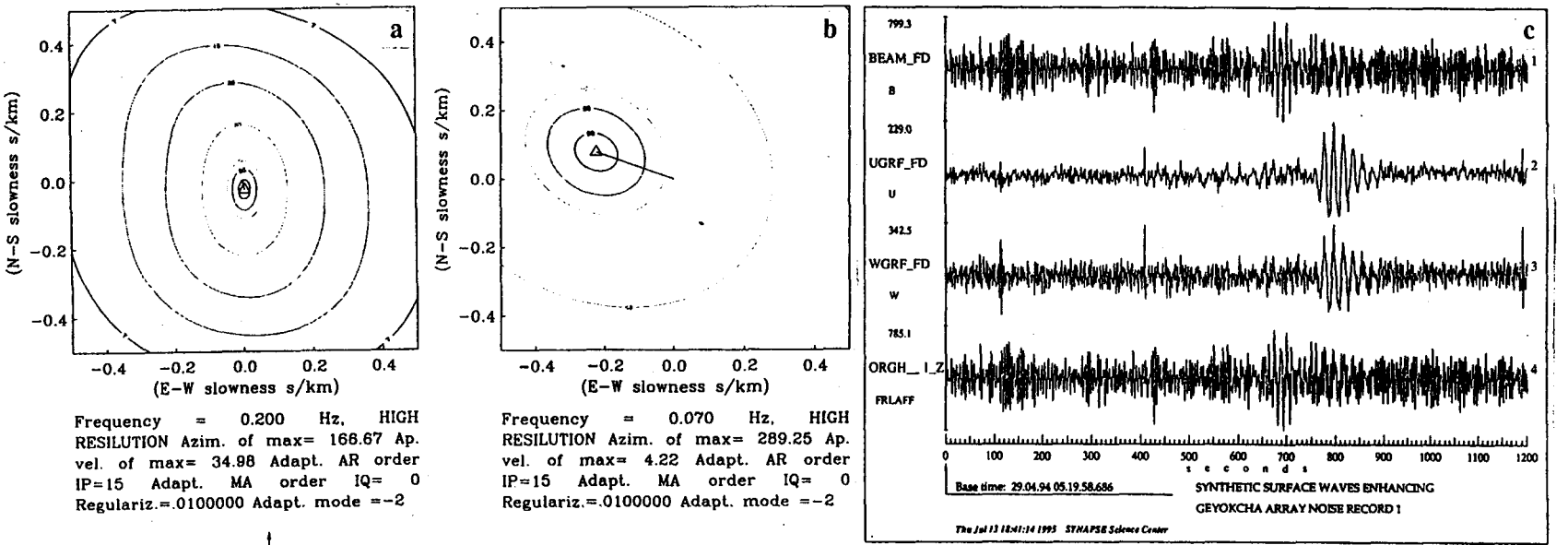

Fig. 5. GEYOKCHA LP noise characteristics: a) b) the F-K maps for different noise components; c) the extraction of simulated explosion surface waves from the real GEYOKCHA noise by the adaptive group filtering (AGF); d) the location of GEYOKCHA VBB sensors; e), f) the noise suppression by the beamforming and AGF in the frequency ranges (0.-10) Hz and (0.-1.) Hz;

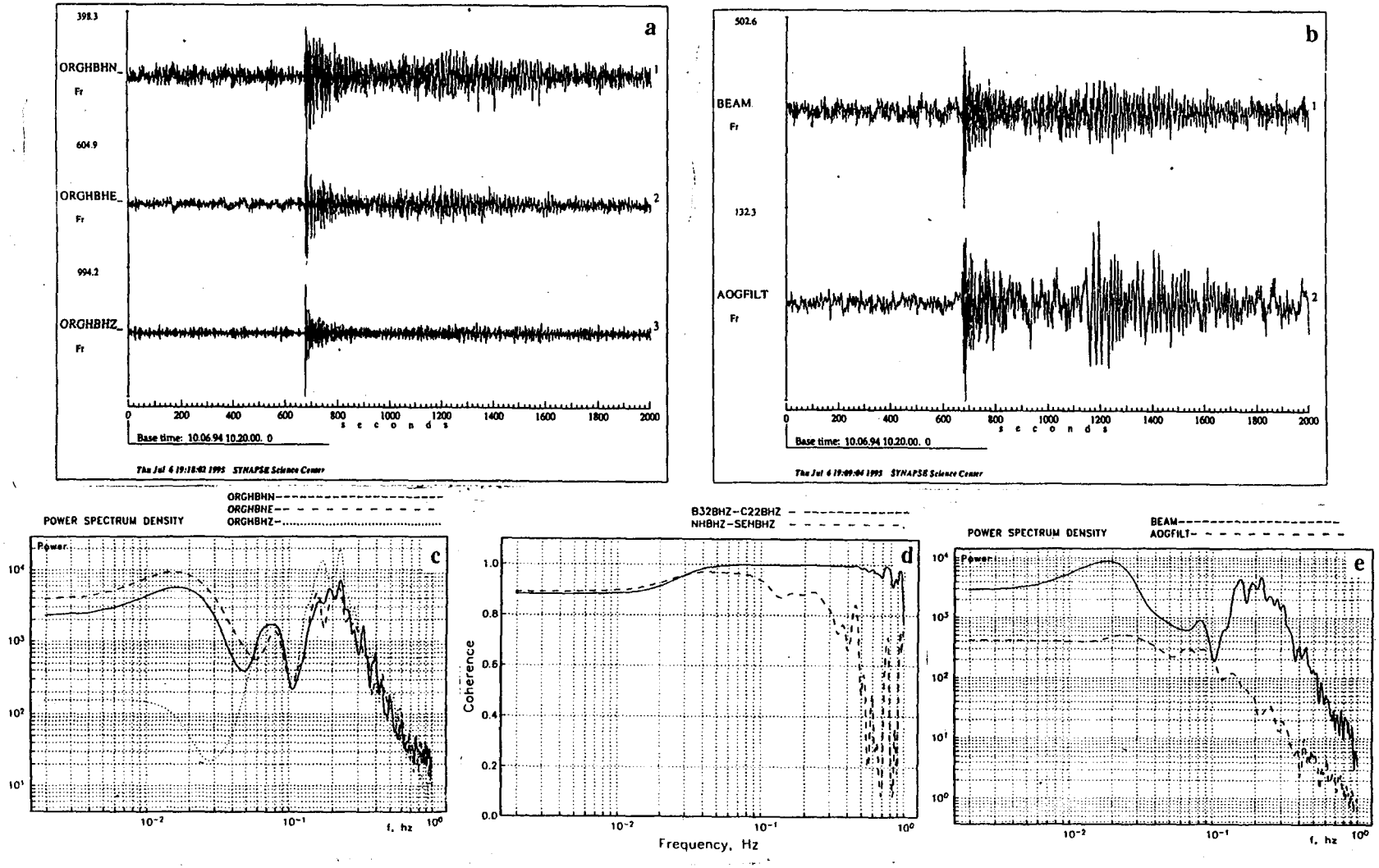

Fig. 6. Extraction of China explosion surface waves using GEYOKCHA VBB 3C records: a) the 3C seismograms of the China explosion; b) the extraction of surface waves by the adaptive group filtering (AGF); c) PSD of 3C noise; d) the noise coherent functions; e) the noise suppression by the AGF